Rogaß, C., Segl, K., Küster, T., Kaufmann, H. (2013): Performance of correlation approaches for the evaluation of spatial distortion reductions. - *Remote Sensing Letters*, *4*, 12, p. 1214-1223.

DOI: http://doi.org/10.1080/2150704X.2013.860565

Performance of correlation approaches for the evaluation of spatial distortion reductions

Christian Rogass*†, Karl Segl, Theres Kuester and Hermann Kaufmann

†Helmholtz Center Potsdam, GFZ German Research Centre for Geosciences, 14473, Potsdam, Germany

Abstract

The analysis of optical remote sensing images often requires a perfect pixel alignment between single bands. Even smallest deviations may degrade the accuracy of subsequent parameter retrieval or lead to the detection of non-existing structures caused by artificial gradients. Hence, a careful pre-processing is essential for minimising spatial non-uniformities such as erroneous co-registration. The results need to be validated and assigned with a quality flag that is unfortunately still not a common practice. In this letter, four broadly used global correlation approaches, namely the two-dimensional Gaussian peak fit, e.g. from Nobach and Honkanen (2005), the poly phase technique from Foroosh et al. (2002), the iterative phase approach from Averbuch and Keller (2002) and its proposed enhancement, were tested for their capacity to serve either as evaluation tool for preceding spatial distortion reductions, e.g. by co-registration, or as global minimiser for generic reduction approaches. For this 8 broadly used test images, 3 Landsat 7 and 3 Landsat 8 samples were artificially sub pixel shifted and degraded by different noise levels resulting in more than 200,000 noise and shift scenarios. Additionally, one state-of-the-art approach was enhanced by 50 % on average for all scenarios and by 280 % on average for all non-degraded images. This study indicates that three out of four approaches can serve as evaluation tools for spatial distortion reductions or as global minimiser even for highly degraded images, whereas proposed enhancement offers highest accuracy and the approach from Foroosh offers best overall performance with regard to considered criteria.

1. Introduction

Remote sensing data require precise geometric pre-processing of bands and images. Remaining spatial non-uniformities, such as erroneous co-registration, can cause artificial gradients that aggravate succeeding analyses. Often geometric pre-processing is inadequately validated, although highly precise local and global approaches, such as Digital Image Correlation (DIC) techniques, exist. A comprehensive overview on DIC techniques is given by Sutton et al. (2009).

However, if two similar images spatially incise then their correlation is maximised. This can be considered as the basic principle of DIC. If images would be phase correlated, then circular shifts could be considered as parameters of the phase plane equation representing the normalised cross power spectrum between the base and the warp image. If images are cross correlated then circular shifts are represented as the displacement of the central correlation peak of the Fourier inverse of the phase correlation.

Both follow the principle of the Fourier Shift Theorem and can serve either as validation tools for the evaluation of preceding geometric pre-processing or as global minimiser for generic approaches.

In this work, cross correlation is used to detect integer shifts, and phase correlation is used to detect sub-pixel shifts. The phase plane equation of phase correlation can be solved using least squares regressions (LSR), as proposed in Averbuch and Keller (2002).
However, three broadly used sub-pixel precise DIC techniques and one enhancement were tested as pre-processing validation tools. Those are the two-dimensional Gaussian peak fit (Argyriou and Vlachos 2006; Debella-Gilo and Kääb 2011; Nobach and Honkanen 2005), the poly phase technique from Foroosh et al. (2006), the iterative phase approach from Averbuch and Keller (2002) and its proposed enhancement. Other modern techniques, from e.g Stone et al. (2001); Tzimiropoulos et al. (2011), were not compared due to the overlap of compared methods and used samples.
The 2D Gaussian peak fit approximates the cross correlation peak by a two-dimensional Gaussian using least squares adjustment. The centre of the Gaussian corresponds to the sub-pixel shifts. The poly phase technique of Foroosh et al. (2002) incorporates information on coherent peaks of the cross correlation matrix to estimate sub-pixel shifts and provides a closed-form analytical solution using poly phase decomposition. The approach from Averbuch and Keller (2002) approximates the sub-pixel shifts as parameters of the phase plane using iterative least squares adjustment that is highly redundant and was used for proposed enhancement.
To enable an objective evaluation of the performance of tested approaches, more than 200,000 shifting scenarios were used representing 121 different sub-pixel shifts, 14 noise levels and 10 repeats for 14 test images of different origin.

2 Correlation Principles

If an image $\mathbf{I} = \mathbf{I}(x, y)$, where image pixels are indexed using $\mathbf{x} = (x, y)$, is shifted by an arbitrary distance along the *x*-direction, notedΔx, and an arbitrary distance along the *y*-direction, noted Δy, then these shifts noted as $\Delta \boldsymbol{x} = (\Delta x, \Delta y)$ can be related in the frequency domain (Averbuch and Keller 2002; Foroosh et al. 2002; Hoge 2003; Keller et al. 2005; Leprince et al. 2007; Ojansivu and Heikkila 2007; Reddy and Chatterji 1996; Tzimiropoulos et al. 2010; Xie et al. 2003) as follows:

$$\mathcal{F}\{\mathbf{I}(x + \Delta x, y + \Delta y)\} = \hat{\mathbf{f}}(u, v)\mathrm{e}^{\mathrm{i}(u\Delta x + v\Delta y)} \tag{1}$$

where $\mathrm{i} = \sqrt{-1}$, $\mathcal{F}$ denotes the Fourier transform, $\hat{\mathbf{f}}$ the Fourier transformed image, u and v are the corresponding frequency variables. Referring the base image to as $\mathbf{I}_1$ and the warped image to as $\mathbf{I}_2$, which share a compact support (spatial overlap), gives the following equation for the cross correlation matrix $\mathbf{C}_{\mathrm{spat}}$ in the spatial domain and for phase correlation matrix $\mathbf{C}_{\mathrm{freq}}$ in the frequency domain (Keller et al. 2005):

$$\mathbf{C}_{\mathrm{spat}} = \mathcal{F}^{-1}\{\mathbf{C}_{\mathrm{freq}}\} = \mathcal{F}^{-1}\left\{\frac{\hat{\mathbf{f}}_1\hat{\mathbf{f}}_2^*}{|\hat{\mathbf{f}}_1||\hat{\mathbf{f}}_2^*|}\right\} \tag{2}$$

where $\mathcal{F}^{-1}$ denotes the inverse Fourier transform, $\hat{\mathbf{f}}_1$ the Fourier transform of $\mathbf{I}_1$ and $\hat{\mathbf{f}}_2^*$ the complex conjugate of the Fourier transform of $\mathbf{I}_2$. To estimate integer shifts between $\mathbf{I}_1$ and $\mathbf{I}_2$, the maximum peak in the cross correlation matrix $\mathbf{C}_{\mathrm{spat}}$ is estimated as described in Keller et al. (2005):

$$\Delta \boldsymbol{x} = \mathrm{argmax}\, \mathbf{C}_{\mathrm{spat}} \tag{3}$$

In the following, an adaption of the approaches described in Averbuch and Keller (2002); Keller et al. (2005) is presented that is able to estimate sub-pixel shifts in the frequency domain, i.e. the phase plane of $\mathbf{C}_{\mathrm{freq}}$ will be analysed. The integer shifts have been estimated by solving equation (3) and assumed to have been corrected beforehand to provide precise compact support for integer pixels. In Averbuch and Keller (2002); Keller et al. (2005), the sub-pixel shifts $\Delta\boldsymbol{x}$ are directly estimated by iteratively applying a weighted least squares regression (IWLSR) to the following equation:

$$-\mathrm{i}\ln C(\mathbf{u}) = -\mathrm{i}\ln\left|\hat{\mathbf{f}}\right| - \boldsymbol{\varphi} = u\Delta x + v\Delta y \ \wedge\ \boldsymbol{\varphi} = \tan^{-1}\frac{\Im(\mathbf{C}_{\mathrm{freq}})}{\Re(\mathbf{C}_{\mathrm{freq}})} \tag{4}$$

where $\Im$ and $\Re$ denote the imaginary and real parts of the phase correlation $\mathbf{C}_{\mathrm{freq}}$ and $\wedge$ the logical conjunction. The amplitude term of equation (4) $-\mathrm{i}\ln\left|\hat{\mathbf{f}}\right|$ implies no sub-pixel-related phase information. Therefore, this term vanishes in the process of IWLSR differentiation leading to a regression between phase $\boldsymbol{\varphi}$ and $u\Delta x + v\Delta y$. In Averbuch and Keller (2002), the phase estimation is conducted as follows:

1. Estimation of the sub-pixel shifts $\Delta\boldsymbol{x}$ by applying IWLSR
2. Definition of compact support and sub-pixel shifting of estimated shifts from 1.
3. Repeat all until a stopping criterion is reached (here, 10^{-6}).

According to Keller et al. (2005), the solution of equation (4) may be inaccurate due to aliasing and phase wrapping.

3 Enhancement of robustness and convergence

In the following, an adaption of Averbuch and Keller (2002); Keller et al. (2005) that aims to reduce the uncertainties in phase unwrapping and the impacts of aliasing and on increasing the overall registration accuracy is presented. In principle, the accuracy of phase estimation is significantly altered if White Gaussian Noise (WGN, Leprince et al. 2007) is present. Hence, the incorporation of noise information in each single phase assessment step may improve the final registration.

However, in this work, a Gaussian function multiplied by the squared residuals vector was selected as the primary weighting function of IWLSR to incorporate the uncertainties in the phase estimation themselves. The Gaussian function incorporates both the loss of relevant signal information distant from the phase correlation matrix centre and the presence of noise. WGN is addressed by relating the sigma of the Gaussian function to the minimum SNR (signal-to-noise ratio) of the base and the warp image. Consequently, a high SNR leads to a broad Gaussian; additionally, more signal information can be incorporated, and vice versa. In the first iteration, the Gaussian can be solely used as a weighting function. This step is crucial because it is assumed that the farther the phase information is from the phase correlation centre, the more noise affects the assessment.

There exists a variety of approaches to quickly assess the SNR. In this work, uncorrelated White Gaussian Noise (WGN, Leprince et al. 2007) was assumed so that the SNR could be expressed as the ratio between the mean of the image and the standard deviation of the difference of the image and its median smoothed representation. This assumption leads to a permanent weighting, whereas the first iteration may predominately affect succeeding assessments. This gives the following equation (5) for the weighting:

$$\mathbf{P}^{j+1} = \frac{\mathbf{w}^j \mathrm{e}^{-\frac{(x-x_0)^2+(y-y_0)^2}{2(\mathrm{SNR})^2}}}{2\pi(\mathrm{SNR})^2} \wedge \mathrm{SNR} = \mathrm{argmin}\left(\frac{\bar{\mathbf{I}}_1}{\sigma(\mathbf{I}_1 - \mathrm{med}(\mathbf{I}_1))}, \frac{\bar{\mathbf{I}}_2}{\sigma(\mathbf{I}_2 - \mathrm{med}(\mathbf{I}_2))}\right) \quad (5)$$

where $\mathbf{P}^{j+1}$ is the final weighting matrix for iteration *j*+1, $\mathbf{w}^j$ the weighting matrix of the previous iteration as function of the previous residuals, *x* and *y* the coordinates in the Gaussian windows, x_0 and y_0 the centre coordinates of the Gaussian window, $\bar{\mathbf{I}}_1$ and $\bar{\mathbf{I}}_2$ the image averages and med the two-dimensional median operator and σ is the standard deviation.

In addition, the IWLRS was conducted in a graduated manner, i.e., the results of the foregoing iteration were used to improve the unknown parameters. Thus, both the convergence speed of the phase assessment and the estimation accuracy are improved because noisy information is suppressed. Further improvements are observed if the phase correlation matrix is additionally smoothed. The impact of the smoothing on the phase estimation varies with the image content and is often significantly lower than the SNR and residuals related Gaussian weighting. According to various tests, a Boxcar with a filter size of 5 x 5 works best and might be appropriate for most cases. This gives the new final equation (6) for the design matrix of the least squares solution:

$$\boldsymbol{\varphi}_{\mathrm{fil}}^j = -\boldsymbol{\varphi}^j * \mathbf{H} \wedge \mathbf{A}^{j+1} = \boldsymbol{\varphi}_{\mathrm{fil}}^j \circ \left(\mathbf{1}_{2,n} + \Delta \boldsymbol{x}^j \otimes \mathbf{1}_n\right) \quad (6)$$

where $\boldsymbol{\varphi}_{\mathrm{fil}}^j$ is the convolved phase $\boldsymbol{\varphi}^j$ of iteration j, $\mathbf{H}$ the filter matrix, * the convolution operator, $\mathbf{A}^{j+1}$ is the design matrix of iteration *j*+1, ∘ the Hadamard product, $\mathbf{1}_{2,n}$ a matrix of width 2 and length *n* valued 1, $\Delta \boldsymbol{x}^j$ the shift vector of iteration *j*, $\mathbf{1}_n$ a vector of width *n* valued 1 and ⊗ the dyadic product.

Hence, the following enhancements were implemented in the approach reported in Averbuch and Keller (2002); Keller et al. (2005):

1. Integer shift estimation in the spatial domain, hence no phase unwrapping is necessary
2. SNR and residuals related Gaussian weighting to reduce aliasing and impact of noise
3. Graduated approach to improve least squares regression and to suppress outliers
4. Spatial smoothing of the phase correlation matrix

All other steps in the processing scheme of Averbuch and Keller (2002) remained unchanged.

4 Experimental results and discussion

To evaluate the performance of all approaches, eight images of the Signal and Image Processing Institute (SIPI) of the University of California (Weber 1997), three Landsat 7 (L7) subsets and three Landsat 8 (L8) subsets were selected, extracted (Landsat subsets) or resampled (only SIPI images) to a broadly used image size of 512 x 512 pixels to be comparable with other approaches. The SIPI images are broadly used for testing image processing approaches, e.g. fig. 1 (*g*) in Foroosh et al. 2002, although the origin is lost. The L7 and L8 scenes were acquired over Phoenix, Arizona at 26.06.2013 and 18.06.2013 (Scene IDs: LE70370372013177EDC00 and LC80370372013169LGN00). The processing level of the Landsat scenes is L1 radiance geo-referenced and terrain corrected, whereby each panchromatic subset incorporates an average ground sampling distance of 15 m and an image size of 7.68 x 7.68 km (fig. 1 (*i*) and (*l*) west to Phoenix, fig. 1 (*j*) and (*m*) northwest to Phoenix, fig 1 (*k*) and (*n*) southwest to Phoenix). Multi-channel images were summed along their

spectral axis. All images were linear scaled to have floating point values between 0.0 and 255.0 (figure 1) to enable a consistent value range without performing bit quantization.

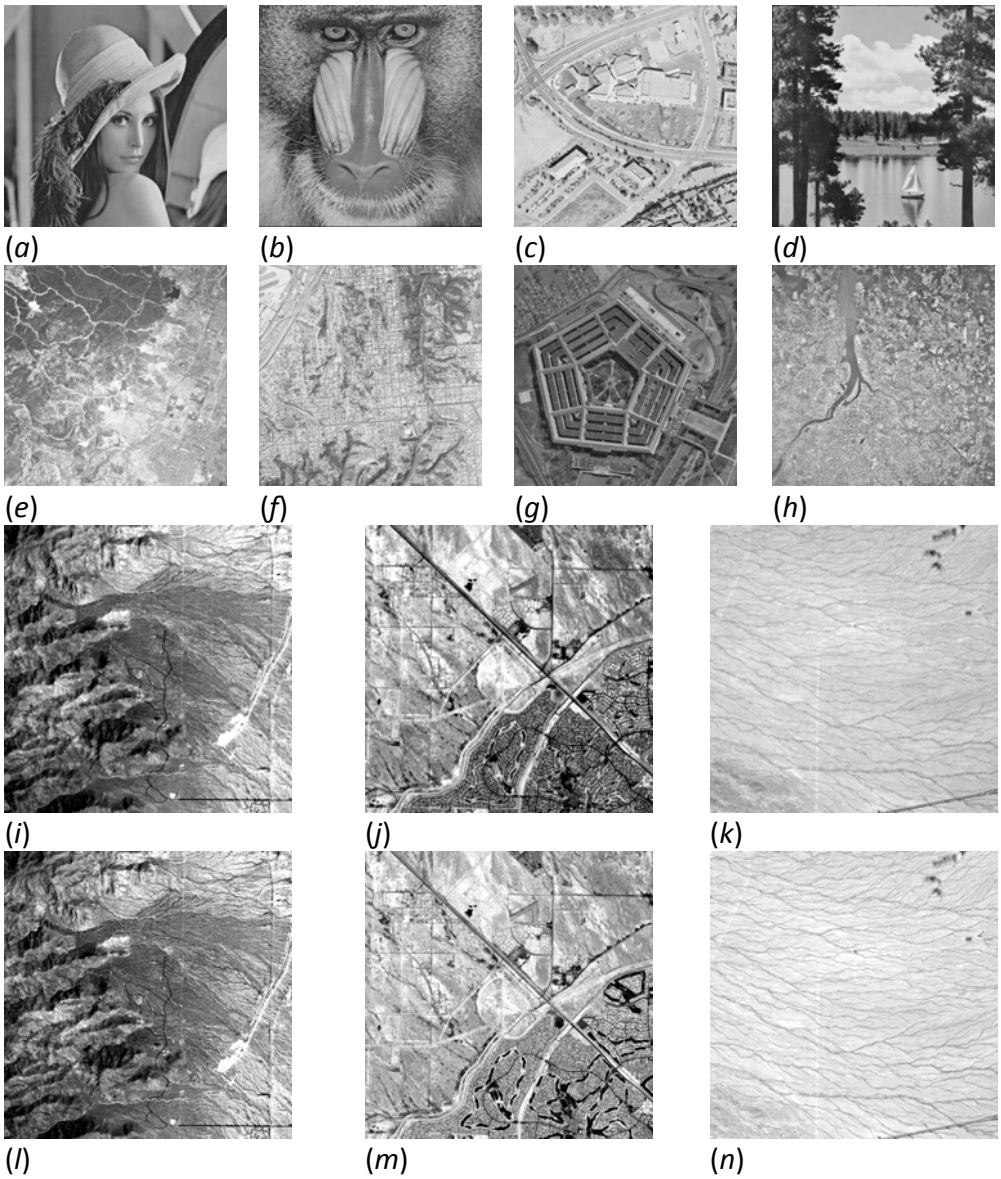

Figure 1. Image samples considered: (a) 'Lenna', (b) 'Mandrill', (c) 'Aerial', (d) 'Sailboat on lake', (e) 2.1.06 'Woodland', (f) 2.1.12 'San Diego', (g) 3.2.25 'Pentagon', (h) wash-ir – 'Washington, D.C.', (i) 'L7 Phoenix 1 medium contrast', (j) 'L7 Phoenix 2 high contrast',(k) 'L7 Phoenix 3 low contrast',(l) 'L8 Phoenix 1 medium contrast', (m) 'L8 Phoenix 2 high contrast' and (n) 'L8 Phoenix 3 low contrast'

Then, different registration scenarios were simulated by conducting artificial sub-pixel shifts (according equation 1; avoids sampling according to Averbuch and Keller 2002) and adding White Gaussian Noise (Box and Muller 1958) for degradations (figure 2) as suggested in Leprince et al. (2007) and to be comparable with inspected approaches. Additionally, the performance of the artificial sub-pixel shifting approach was tested and the necessity for apodization evaluated (Leprince et al. 2007; Reu 2011). For this, 8 checkerboards of different size ranging from 32 to

4096 square pixels (2^5 – 2^8 square pixels) were artificially shifted analogous to test images (5). Those tests revealed an error rate for this artificial sub-pixel shifting approach and rectangular apodization of 2.9^{-5} % (σ=1.2^{-5} %) on average for all maximum deviations and, hence, it was assumed to be appropriate for simulations (used sampling rate of 1 gives the same approach as in Foroosh et al. (2002); Stone et al. (2001); Tzimiropoulos et al. (2011). In the following (equation 7), the WGN degradations vector $\boldsymbol{\sigma}_{\text{noise}}$ (which always has a zero mean and scenario-dependent standard deviation σ) and all shift vectors $\Delta\boldsymbol{x}$ and $\Delta\boldsymbol{y}$ are listed:

$$\boldsymbol{\sigma}_{\text{noise}} = [0, 0.1, 0.025, 0.05, 0.1, 0.25, 0.5, 1, 2.5, 5, 10, 20, 50, 100]$$
$$\Delta\boldsymbol{x} = [-0.5, -0.4, -0.3, -0.2, -0.1,0,0.1,0.2,03.,0.4,0.5] \wedge \Delta\boldsymbol{y} = \Delta\boldsymbol{x} \qquad (7)$$

For each image and each scenario, all four approaches considered were applied and evaluated according to an absolute sub-pixel error with the same noise degradation. In total, 11x11 shifts, 14 noise levels and 10 repeats, representing 16940 different scenarios for each image and method, were performed (see figure 2).

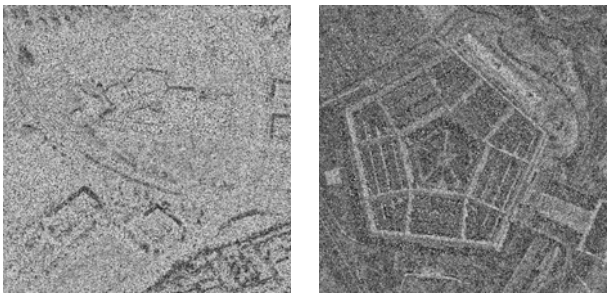

(*a*) (*b*)

Figure 2. Image degradation with uncorrelated WGN σ=50 of (a) 'Aerial' and (b) 'Pentagon'

In each scenario, both the image and its shifted representation were degraded by different noise matrices with the same WGN standard deviation. This process was repeated 10 times using different noise matrices with the same standard deviation before the results were averaged. Then, for each noise scenario but all 121 shifts, the average pixel errors were computed which are presented in figure 3.

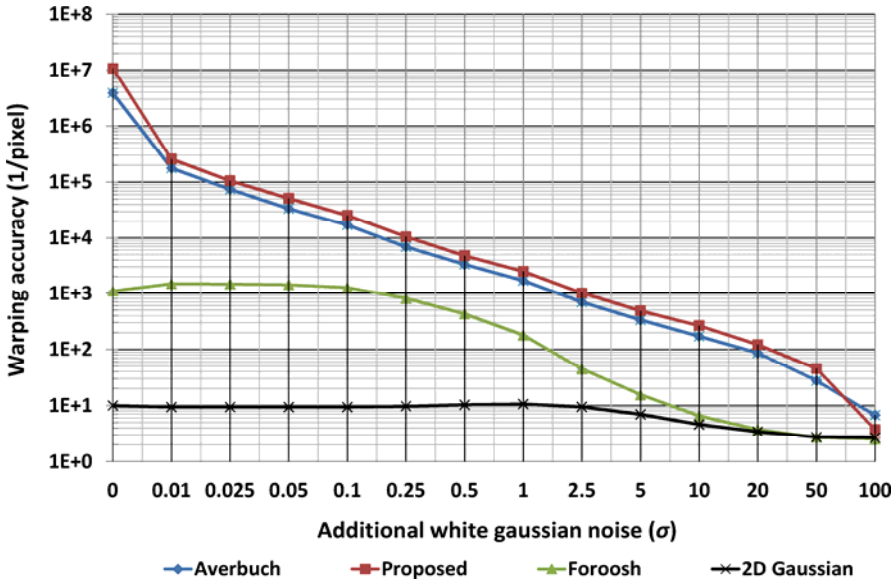

Figure 3. Averaged warping accuracies for all degradations, σ=0 original images, log-log-plot

The figure shows that all evaluated approaches achieve sub-pixel precision in different noise scenarios even for the $\boldsymbol{\sigma}_{\mathrm{noise}}(14) = 100$ scenario. It also shows that proposed, the approach from Averbuch and Foroosh approach significantly perform better than the 2D Gaussian fitting approach. Additionally, the approach from Averbuch and the proposed approach significantly perform better than the poly phase approach of Foroosh. However, the proposed approach outperforms all other investigated approaches except for the $\boldsymbol{\sigma}_{\mathrm{noise}}(14)$ scenario, in which the 2D Gaussian fit and the Foroosh approach clearly perform better. The presented revised approach shows a performance enhancement of approximately 50 % on average (except for the $\boldsymbol{\sigma}_{\mathrm{noise}}(14)$ scenario) compared to the approach from Averbuch for all images and all scenarios and of approximately 280 % on average for all non-degraded images. This is additionally shown in table 1, where the accuracy improvements are presented as factors with respect to the considered methods.

Method	**Improvement Factor**		
	White Gaussian Noise *σ*		
	0 (original)	**0.01-1**	**2.5-100**
Averbuch	2.8	1.4	1.3
Foroosh	2799	38	17
Gaussian	410565	5490	37

Table 1. Averaged ratios of sub-pixel accuracies between proposed and evaluated approaches – factors of improvement

The results show that the proposed method clearly outperforms all other methods, except for the highest-noise case, for which the assumed WGN is negligible for modern image sensors. Considering only the original images, both the enhancement and its precursor significantly outperform all other considered approaches. Except for the $\boldsymbol{\sigma}_{\mathrm{noise}}(14)$ scenario all approaches perform equally on average for Landsat 7 and Landsat 8 that indicates a high SNR of both sensors.
To avoid relying on a single criterion for an overall benchmark, additional criteria were included. These are in a subjectively ranked order the accuracy, the computational speed, the implementation simplicity and the minimum window size. In figure 4 the average computational speed is shown. It indicates that iterative approaches such as the proposed (0.65 s per image on average) or the approach from Averbuch (0.46 s per image on average) are approximately 10 times slower as the approach from Foroosh (0.047 s per image on average) and as the 2D Gaussian fit (0.052 s per image on average) whereby computational time increases if images become noisier.

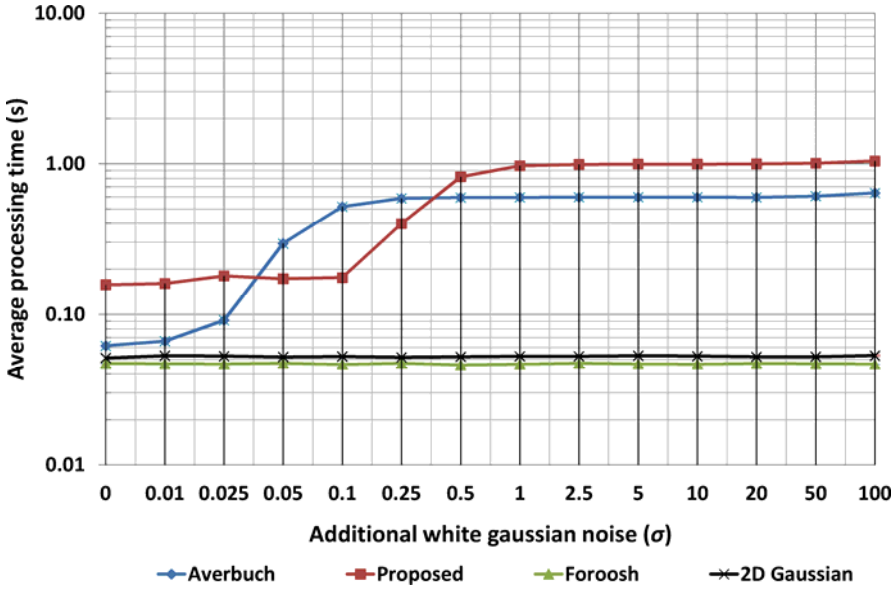

Figure 4. Averaged warping time for all degradations, σ=0 original images, log-log-plot

The implementation simplicity may be also an important criterion. With regard to conducted implementation efforts the approach of Foroosh would be ranked according its implementation simplicity as first, 2D Gaussian fit as second, the approach from Averbuch as third and the proposed approach as fourth. Additionally, the minimum window size in which the correlation can be performed may be important for some applications, because some spatial distortions such as short-time attitude variations induce non-linear distortions even in small pixel windows. With regard to conducted optimisation efforts to achieve for each approach the best result, the approach from Foroosh and the 2D Gaussian fit approach (3 x 3 sized window possible) would be ranked according the minimum window size as first and the approach from Averbuch and the proposed approach as second.
In the following table an overall ranking is given that enables a specific selection of the approach depending on application. If only accuracy is selected as criterion the proposed approach outperforms all other approaches. If all criteria are selected and equally weighted the approach of Foroosh is the best inspected approach.

Method	**Ranking**			
			Criterion	
	Accuracy	**Speed**	**Implementation simplicity**	**Minimum window size**
Averbuch	2	3	3	2
Proposed	1*	4	4	2
Foroosh	3	1*	1*	1*
2D Gaussian	4	2	2	1*

* Highest rank

Table 2. Overall ranking of investigated approaches according some criteria

5 Conclusion

Assuming images of modern sensors incorporating uncorrelated WGN of no more than $\boldsymbol{\sigma}_{\mathrm{noise}}(11) = 10$ the proposed approach as well as the approaches from Averbuch and Foroosh appear to be noise robust and, hence, may serve as evaluation tool for the reduction of spatial

non-uniformities or as global minimiser. Additionally, an enhancement of the approach from Averbuch that enables higher accuracies compared to those of the original approach was presented. In the case of very high image noise, the proposed approach should be combined with the approach of Averbuch or Foroosh to achieve higher accuracy. However, inspected approaches except the 2D Gaussian fit approach appear to be more precise than typical pre-processing related distortion reductions (often above 1/100 pixel) and hence may serve as evaluation tools. Depending on application the approach of Foroosh appears to be general applicable and achieves an accuracy of better than 1/1000 pixel in most scenarios. It appears that this approach might be generally used to detect local distortions because of the minimum window size of 3 x 3 pixels. It follows from this that the proposed approach and the approach from Averbuch could be applied globally and the approach of Foroosh locally. This would enable the detection of remaining local and global spatial disjoints smaller than 1/10 pixel as well as image registration of noisy images.

Acknowledgements

This work was funded by the German Federal Ministry of Economics and Technology (BMWI 50EE1012/EnMAP) within the framework of EnMAP (Environmental Mapping and Analysis Program). We thank both U.S. institutions, the UC SIPI and NASA's Land Processes Distributed Active Archive Center (LP DAAC), for providing image samples and Landsat satellite images. We are grateful to anonymous reviewers and the Editor for their constructive and insightful comments that helped to improve the quality of the manuscript.

6 References

Argyriou, V. & Vlachos, T., 2006. A study of sub-pixel motion estimation using phase correlation. In M. Chantler, B. Fisher, & M. Trucco, eds. In Proc. of the British Machine Vision Conference 2006, Edinburgh, UK, September 4-7. BMVA Press, pp. 387–396.

Averbuch, A. & Keller, Y., 2002. FFT based image registration. In Proc. of the 2002 IEEE International Conference on Acoustics, Speech, and Signal Processing (ICASSP), Orlando, Florida, USA, May 13-17, IEEE, pp. 3608-3611.

Box, G. & Muller, M.E., 1958. A note on the generation of random normal deviates. *Annals of Mathematical Statistics*, 29, pp.610–611.

Debella-Gilo, M. & Kääb, A., 2011. Sub-pixel precision image matching for measuring surface displacements on mass movements using normalized cross-correlation. *Remote Sensing of Environment*, 115, pp.130–142.

Foroosh, H., Zerubia, J.B. & Berthod, M., 2002. Extension of phase correlation to subpixel registration*., IEEE Transactions on Image Processing*, 11, pp.188–200.

Hoge, W.S., 2003. A subspace identification extension to the phase correlation method [MRI application]*., IEEE Transactions on Medical Imaging*, 22, pp.277–280.

Keller, Y., Averbuch, A. & Israeli, M., 2005. Pseudopolar-based estimation of large translations, rotations, and scalings in images*., IEEE Transactions on Image Processing*, 14, pp.12–22.

Leprince, S. et al., 2007. Automatic and precise orthorectification, coregistration, and subpixel correlation of satellite images, application to ground deformation measurements*., IEEE Transactions on Geoscience and Remote Sensing*, 45, pp.1529–1558.

Nobach, H. & Honkanen, M., 2005. Two-dimensional Gaussian regression for sub-pixel displacement estimation in particle image velocimetry or particle position estimation in particle tracking velocimetry. *Experiments in fluids*, 38, pp.511–515.

Ojansivu, V. & Heikkila, J., 2007. Image Registration Using Blur-Invariant Phase Correlation. *IEEE Signal Processing Letters,* 14, pp.449–452.

Reddy, B.S. & Chatterji, B., 1996. An FFT-based technique for translation, rotation, and scale-invariant image registration*., IEEE Transactions on Image Processing*, 5, pp.1266–1271.

Reu, P., 2011. Experimental and numerical methods for exact subpixel shifting. *Experimental mechanics*, 51, pp.443–452.

Stone, H.S. et al., 2001. A fast direct Fourier-based algorithm for subpixel registration of images*., IEEE Transactions on Geoscience and Remote Sensing*, 39, pp.2235–2243.

Sutton, M.A., Orteu, J.-J. & Schreier, H.W., 2009. *Image correlation for shape, motion and deformation measurements: basic concepts, theory and applications*, Springer.

Tzimiropoulos, G. et al., 2010. Robust FFT-based scale-invariant image registration with image gradients*., IEEE Transactions on Pattern Analysis and Machine Intelligence*, 32, pp.1899–1906.

Tzimiropoulos, G., Argyriou, V. & Stathaki, T., 2011. Subpixel registration with gradient correlation*., IEEE Transactions on Image Processing*, 20, pp.1761–1767.

Weber, A.G., 1997. *The USC-SIPI Image Database* 5th ed., Los Angeles, CA 90089-2564 USA, 3740 McClintock Ave: University of Southern California, Signal and Image Processing Institute, Department of Electrical Engineering.

Xie, H. et al., 2003. An IDL/ENVI implementation of the FFT-based algorithm for automatic image registration. *Computers & Geosciences*, 29, pp.1045–1055.